

# Autocorrelation function of velocity increments time series in fully developed turbulence

Y.X. HUANG<sup>1,2</sup> <sup>(a)</sup>, F. G. SCHMITT<sup>2</sup> <sup>(b)</sup>, Z.M. LU<sup>1</sup> and Y.L. LIU<sup>1</sup>

<sup>1</sup> *Shanghai Institute of Applied Mathematics and Mechanics, Shanghai University, 200072 Shanghai, China*

<sup>2</sup> *Université des Sciences et Technologies de Lille - Lille 1, CNRS, Laboratory of Oceanology and Geosciences, UMR 8187 LOG, 62930 Wimereux, France*

PACS 05.45.Tp – Time series analysis  
 PACS 02.50.Fz – Stochastic analysis  
 PACS 47.27.Gs – Isotropic turbulence; homogeneous turbulence

**Abstract** – In fully developed turbulence, the velocity field possesses long-range correlations, denoted by a scaling power spectrum or structure functions. Here we consider the autocorrelation function of velocity increment  $\Delta u_\ell(t)$  at separation time  $\ell$ . Anselmet et al. [Anselmet et al. J. Fluid Mech. **140**, 63 (1984)] have found that the autocorrelation function of velocity increment has a minimum value, whose location is approximately equal to  $\ell$ . Taking statistical stationary assumption, we link the velocity increment and the autocorrelation function with the power spectrum of the original variable. We then propose an analytical model of the autocorrelation function. With this model, we prove that the location of the minimum autocorrelation function is exactly equal to the separation time  $\ell$  when the scaling of the power spectrum of the original variable belongs to the range  $0 < \beta < 2$ . This model also suggests a power law expression for the minimum autocorrelation. Considering the cumulative function of the autocorrelation function, it is shown that the main contribution to the autocorrelation function comes from the large scale part. Finally we argue that the autocorrelation function is a better indicator of the inertial range than the second order structure function.

**Introduction.** – Turbulence is characterized by power law of the velocity spectrum [1] and structure functions in the inertial range [2,3]. This is associated to long-range power-law correlations for the dissipation or absolute value of the velocity increment. Here we consider the autocorrelation of velocity increments (without absolute value), inspired by a remark found in Anselmet et al. (1984) [4]. In this reference, it is found that the location of the minimum value of the autocorrelation function  $\Gamma(\tau)$  of velocity increment  $\Delta u_\ell(t)$ , defined as

$$\Delta u_\ell(t) = u(t + \ell) - u(t) \quad (1)$$

of fully developed turbulence with time separation  $\ell$  is approximately equal to  $\ell$ . The autocorrelation function of this time series is defined as

$$\Gamma(\tau) = \langle (V_\ell(t) - \mu)(V_\ell(t - \tau) - \mu) \rangle \quad (2)$$

<sup>(a)</sup>E-mail: yongxianghuang@gmail.com

<sup>(b)</sup>E-mail: francois.schmitt@univ-lille1.fr

34 where  $V_\ell(t) = \Delta u_\ell(t)$ ,  $\mu$  is the mean value of  $V$ , and  $\tau > 0$  is the time lag.

35 This paper mainly presents analytical results. In first section we present the database  
 36 considered here as an illustration of the property which is studied. The next section presents  
 37 theoretical studies. The last section provides a discussion.

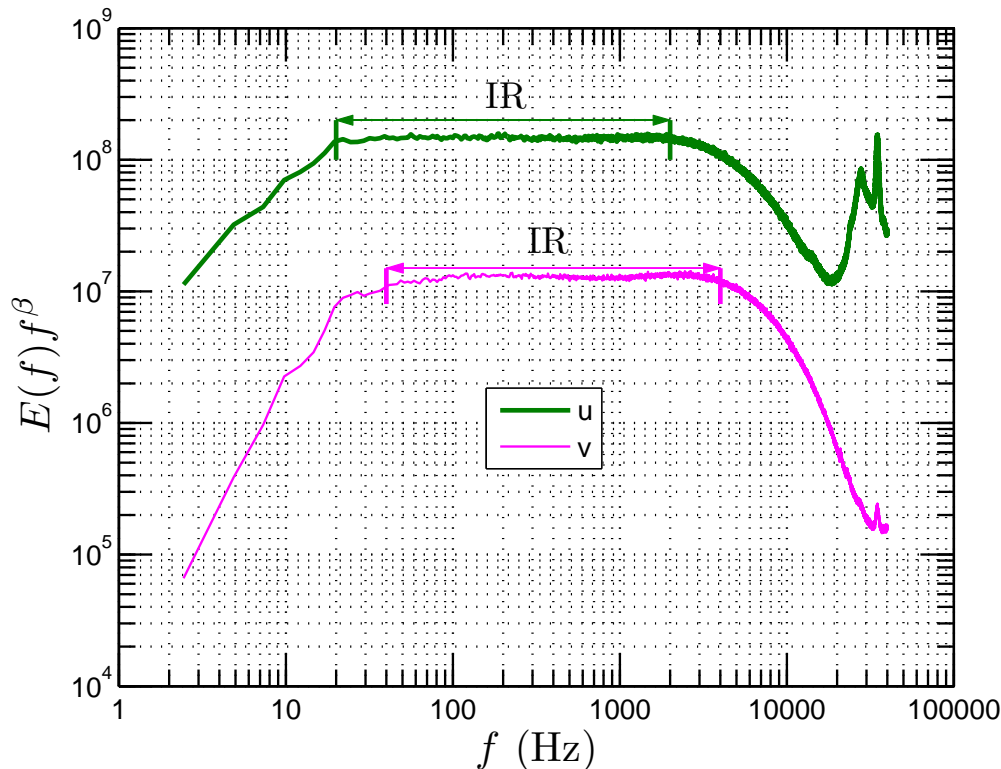


Fig. 1: Compensated spectrum  $E(f)f^\beta$  of streamwise (longitudinal) ( $\beta \simeq 1.63$ ) and spanwise (transverse) ( $\beta \simeq 1.62$ ) velocity, where  $\beta$  is the corresponding power law estimated from the power spectrum. The plateau is observed on the range  $20 < f < 2000$  Hz and  $40 < f < 4000$  Hz for streamwise (longitudinal) and spanwise (transverse) velocity, respectively.

### 38 Experimental analysis of the autocorrelation function of velocity increments.

39 – We consider here a turbulence velocity time series obtained from an experimental homo-  
 40 geneous and nearly isotropic turbulent flow at downstream  $x/M = 20$ , where  $M$  is the mesh  
 41 size. The flow is characterized by the Taylor microscale based Reynolds number  $Re_\lambda = 720$   
 42 [5]. The sampling frequency is  $f_s = 40$  kHz and a low-pass filter at a frequency 20 kHz  
 43 is applied on the experimental data. The sampling time is 30 s, and the number of data  
 44 points per channel for each measurement is  $1.2 \times 10^6$ . We have 120 realizations with four  
 45 channels. The total number of data points at this location is  $5.76 \times 10^8$ . The mean velocity  
 46 is  $12 \text{ ms}^{-1}$ . The rms velocity is 1.85 and  $1.64 \text{ ms}^{-1}$  for streamwise (longitudinal) and span-  
 47 wise (transverse) velocity component. The Kolmogorov scale  $\eta$  and the Taylor microscale  
 48  $\lambda$  are 0.11 mm and 5.84 mm respectively. Let us note here  $T_s = 1/f_s$  time resolution of  
 49 these measurements. This data demonstrates an inertial range over two decades [5], see  
 50 a compensated spectrum  $E(f)f^\beta$  in fig. 1, where  $\beta \simeq 1.63$  and  $\beta \simeq 1.62$  for streamwise  
 51 (longitudinal) and spanwise (transverse) velocity respectively. We show the autocorrelation  
 52 function  $\Gamma_\ell(\tau)$  directly estimated from these data in fig. 2. Graphically, the location  $\tau_o$  of  
 53 the minimum value of each curve is very close to  $\ell$ , which confirms Anselmet's observation

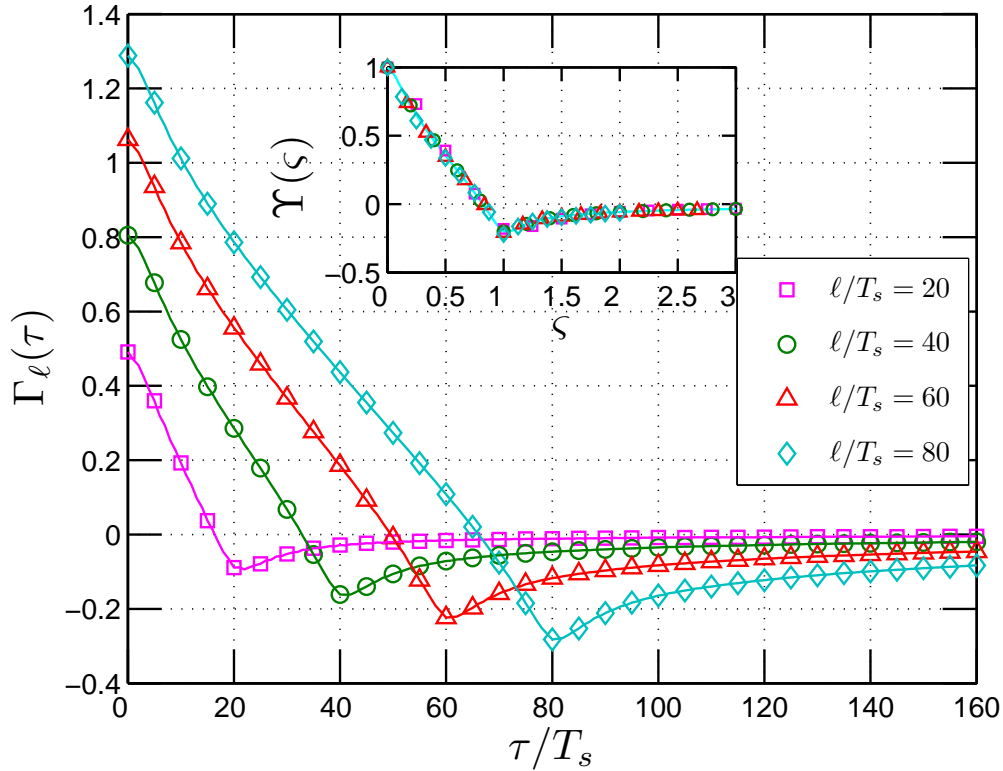


Fig. 2: Autocorrelation function  $\Gamma_\ell(\tau)$  of the velocity increment  $\Delta u_\ell(t)$  estimated from an experimental homogeneous and nearly isotropy turbulence time series with various increments  $\ell$ . The location of the minimum value is very close to the separation time  $\ell$ . The inset shows the rescaled autocorrelation function  $\Upsilon(\varsigma)$ .

54 [4]. Let us define

$$\Gamma_o(\ell) = \min_{\tau} \{\Gamma_\ell(\tau)\} \quad (3)$$

55 and  $\tau_o$  the location of the minimum value

$$\Gamma_o(\ell) = \Gamma_\ell(\tau_o(\ell)) \quad (4)$$

56 We show the estimated  $\tau_o(\ell)$  on the range  $2 < \ell/T_s < 40000$  in fig. 3, where the inertial  
 57 range is indicated by IR. It shows that when  $\ell$  is greater than  $20T_s$ ,  $\tau_o$  is very close to  $\ell$  even  
 58 when  $\ell$  is in the forcing range, in agreement with the remark of Anselmet et al. [4]. In the  
 59 following, we show this analytically.

60 **Autocorrelation function.** — Considering the statistical stationary assumption [3],  
 61 we represent  $u(t)$  in Fourier space, which is written as

$$\hat{U}(f) = \mathcal{F}(u(t)) = \int_{-\infty}^{+\infty} u(t) e^{-2\pi i f t} dt \quad (5)$$

62 where  $\mathcal{F}$  means Fourier transform and  $f$  is the frequency. Thus, the Fourier transform of  
 63 the velocity increment  $\Delta u_\ell(t)$  is written as

$$S_\ell(f) = \mathcal{F}(\Delta u_\ell(t)) = \hat{U}(f)(e^{2\pi i f \ell} - 1) \quad (6)$$

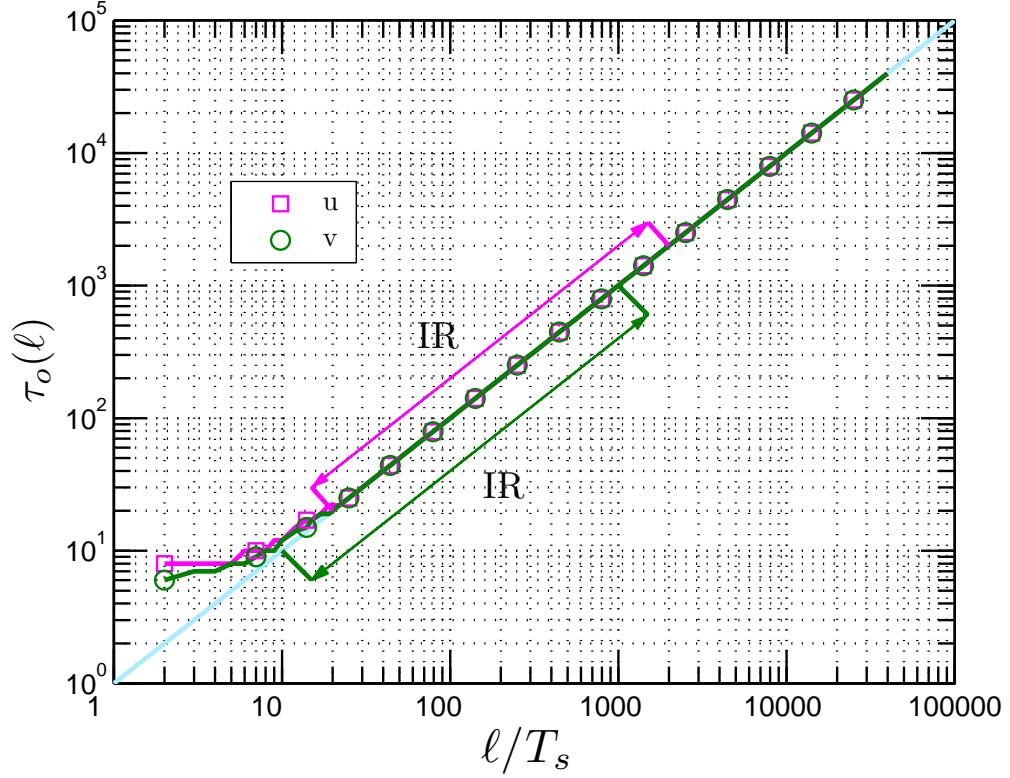


Fig. 3: Location  $\tau_o(\ell)$  of the minimum value of the autocorrelation function estimated from experimental data, where the inertial range is marked as IR. The solid line indicates  $\tau_o(\ell) = \ell$ .

64 where  $\Delta u_\ell(t) = u(t + \ell) - u(t)$ . Hence, the 1D power spectral density function of velocity  
 65 increments  $E_\Delta(f)$  is expressed as

$$E_\Delta(f) = |S_\ell(f)|^2 = E_v(f)(1 - \cos(2\pi f\ell)) \quad (7)$$

66 where  $E_v(f) = 2|\hat{U}(f)|^2$  is the velocity power spectrum [3]. It is clear that the velocity  
 67 increment operator acts a kind of filter, where the frequencies  $f_\Delta = n/\ell$ ,  $n = 0, 1, 2, \dots$ , are  
 68 filtered.

69 Let us consider now the autocorrelation function of the increment. The Wiener-Khinchin  
 70 theorem relates the autocorrelation function to the power spectral density via the Fourier  
 71 transform [3, 6]

$$\Gamma_\ell(\tau) = \int_0^{+\infty} E_\Delta(f) \cos(2\pi f\tau) df \quad (8)$$

72 The theorem can be applied to wide-sense-stationary random processes, signals whose  
 73 Fourier transforms may not exist, using the definition of autocorrelation function in terms  
 74 of expected value rather than an infinite integral [6]. Substituting eq. (7) into the above  
 75 equation, and assuming a power law for the spectrum (a hypothesis of similarity)

$$E_v(f) = cf^{-\beta}, \quad c > 0 \quad (9)$$

76 we obtain

$$\Gamma_\ell(\tau) = c \int_0^{+\infty} f^{-\beta} (1 - \cos(2\pi f\ell)) \cos(2\pi f\tau) df \quad (10)$$

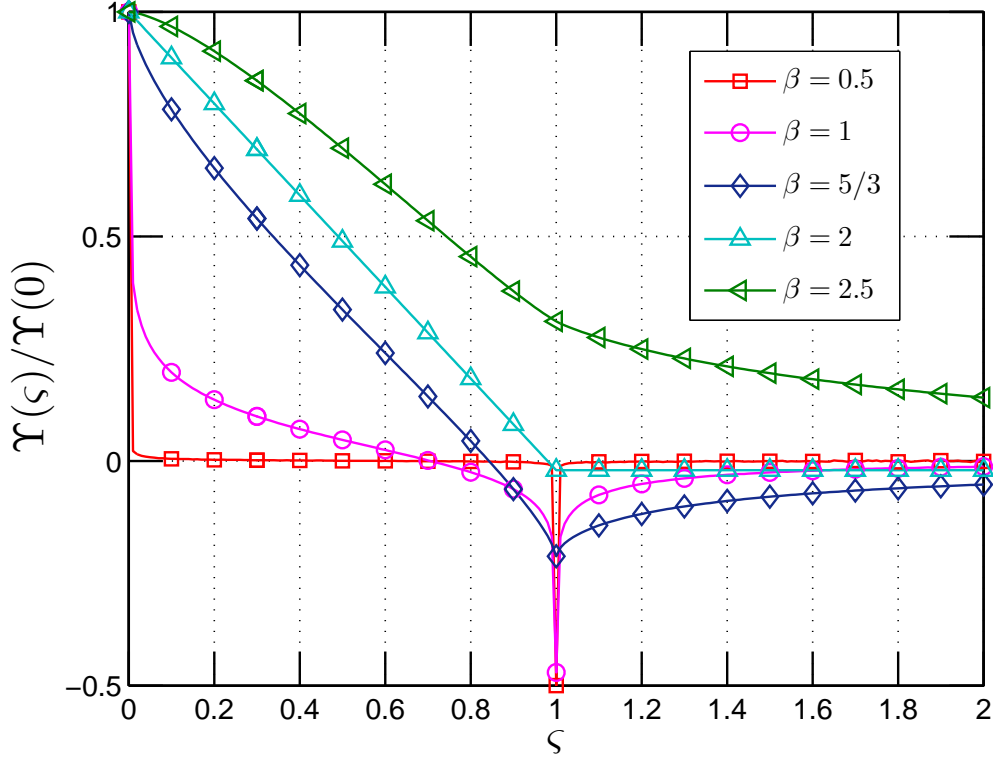


Fig. 4: Numerical solution of the rescaled autocorrelation function  $\Upsilon(\varsigma)$  with various  $\beta$  from 0.5 to 2.5 estimated from eq. (10).

77 The convergence condition requires  $0 < \beta < 3$ . It implies a rescaled relation, using scaling  
 78 transformation inside the integral. This can be estimated by taking  $\ell' = \lambda\ell$ ,  $f' = f\lambda$ ,  
 79  $\tau' = \tau/\lambda$  for  $\lambda > 0$ , providing the identity

$$\Gamma_{\lambda\ell}(\tau) = \Gamma_{\ell}(\tau/\lambda)\lambda^{\beta-1} \quad (11)$$

80 If we take  $\ell = 1$  and replace  $\lambda$  by  $\ell$ , we then have

$$\Gamma_{\ell}(\tau) = \Gamma_1(\tau/\ell)\ell^{\beta-1} \quad (12)$$

81 Thus, we have a universal autocorrelation function

$$\Gamma_{\ell}(\ell\varsigma)\ell^{1-\beta} = \Upsilon(\varsigma) = \Gamma_1(\varsigma) \quad (13)$$

82 This rescaled universal autocorrelation function is shown as inset in fig. 2. A derivative of  
 83 eq. (11) gives  $\Gamma'_{\lambda\ell}(\tau) = \Gamma'_{\ell}(\tau/\lambda)\lambda^{\beta-2}$ . The minimum value of the left-hand side is  $\tau = \tau_o(\lambda\ell)$ ,  
 84 verifying  $\Gamma'_{\lambda\ell}(\tau_o(\lambda\ell)) = 0$  and for this value we have also  $\Gamma'_{\ell}(\tau_o(\lambda\ell)/\lambda) = 0$ . This shows that  
 85  $\tau_o(\ell) = \tau_o(\lambda\ell)/\lambda$ . Taking again  $\ell = 1$  and  $\lambda = \ell$ , we have

$$\tau_o(\ell) = \ell\tau_o(1) \quad (14)$$

86 Showing that  $\tau_o(\ell)$  is proportional to  $\ell$  in the scaling range (when  $\ell$  belongs to the inertial  
 87 range). With the definition of  $\Gamma_o(\ell) = \Gamma_{\ell}(\tau_o(\ell))$  we have, also using eq. (11), for  $\tau = \tau_o(\lambda\ell)$ :

$$\begin{aligned} \Gamma_{\lambda\ell}(\tau_o(\lambda\ell)) &= \Gamma_{\ell}(\tau_o(\lambda\ell)/\lambda)\lambda^{\beta-1} \\ &= \Gamma_{\ell}(\tau_o(\ell))\lambda^{\beta-1} \end{aligned} \quad (15)$$

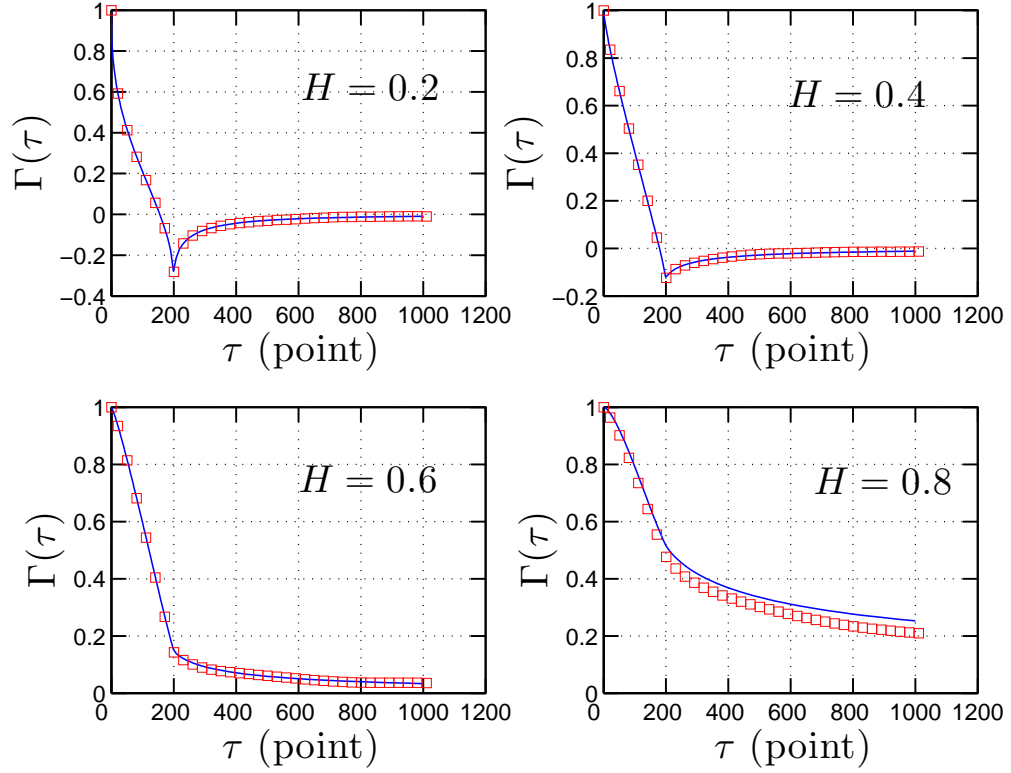


Fig. 5: Comparison of the autocorrelation function, which is predicted by eq. (20) (solid line) and estimated from fBm simulation ( $\square$ ) with  $\ell = 200$  points.

88 Hence  $\Gamma_o(\lambda\ell) = \lambda^{\beta-1}\Gamma_o(\ell)$  or

$$\Gamma_o(\ell) = \Gamma_o(1)\ell^{\beta-1} \quad (16)$$

89 We now consider the location  $\tau_o(1)$  of the autocorrelation function for  $\ell = 1$ . We take  
90 the first derivative of eq. (10), written for  $\ell = 1$

$$\mathcal{P}(\tau) = \frac{d\Gamma_1(\tau)}{d\tau} = - \int_0^{+\infty} f^{1-\beta}(1 - \cos(2\pi f)) \sin(2\pi f\tau) df \quad (17)$$

91 where we left out the constant in the integral. The same rescaling calculation leads to the  
92 following expression

$$\begin{aligned} \mathcal{P}(\tau) &= [(1 + 1/\tau)^{\beta-2} + (1 - 1/\tau)^{\beta-2} - 2] M/2, \tau \neq 1 \\ \mathcal{P}(\tau) &= (2^{\beta-3} - 1) M, \quad \tau = 1 \end{aligned} \quad (18)$$

93 where  $M = \int_0^{+\infty} x^{1-\beta}(1 - \cos(2\pi x)) \sin(2\pi x\tau) dx$  and  $M > 0$  [7]. The convergence condition  
94 requires  $1 < \beta < 4$ . When  $\beta < 2$ , one can find that both left and right limits of  $\mathcal{P}(1)$  are  
95 infinite, but the definition of  $\mathcal{P}(1)$  in eq. (17) is finite. Thus  $\tau = 1$  is a second type  
96 discontinuity point of eq. (17) [8]. It is easy to show that

$$\begin{cases} \mathcal{P}(\tau) < 0, \tau \leq 1 \\ \mathcal{P}(\tau) > 0, \tau > 1 \end{cases} \quad (19)$$

97 It means that  $\mathcal{P}(\tau)$  changes its sign from negative to positive when  $\tau$  is increasing from  
98  $\tau < 1$  to  $\tau > 1$ . In other words the autocorrelation function will take its minimum value at  
99 the location where  $\tau$  is exactly equal to 1. We thus see that  $\tau_o(1) = 1$  and hence  $\tau_o(\ell) = \ell$   
100 (eq. (14)).

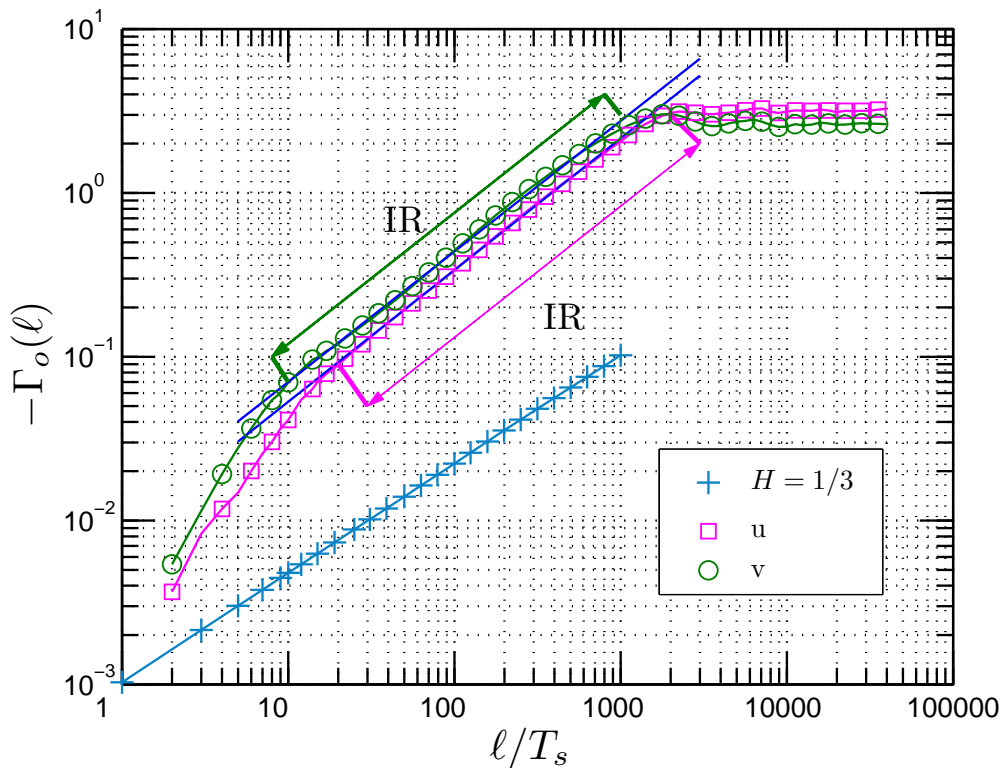


Fig. 6: Representation of the minima value  $\Gamma_o(\ell)$  of the autocorrelation function estimated from synthesized fBm time series with  $H = 1/3$  (+), and the experimental data for streamwise (longitudinal) ( $\square$ ) and spanwise (transverse) ( $\circ$ ) turbulent velocity components, where the corresponding inertial range is denoted as IR. Power law behaviour is observed with scaling exponent  $\beta - 1 = 2/3$  and  $\beta - 1 = 0.78 \pm 0.04$  for fBm and turbulent velocity, respectively.

101 **Numerical validation.** – There is no analytical solution for eq. (10). It is then  
 102 solved here by a proper numerical algorithm. We perform a fourth order accurate Simpson  
 103 rule numerical integration of eq. (10) on range  $10^{-4} < f < 10^4$  with  $\ell = 1$  for various  $\beta$   
 104 with step  $\Delta f = 10^{-6}$ . We show the rescaled numerical solutions  $\Upsilon(\zeta)$  for various  $\beta$  values  
 105 in fig. 4. Graphically, as what we have proved above, the location  $\tau_o(1)$  of the minimum  
 106 autocorrelation function is exactly equal to 1 when  $0 < \beta < 2$ .

107 For the fBm, the autocorrelation function of the increments is known to be the following  
 108 [9]

$$\Gamma_\ell(\tau) = \frac{1}{2} \{ (\tau + \ell)^{2H} + |\tau - \ell|^{2H} - \tau^{2H} \} \quad (20)$$

109 where  $\tau \geq 0$ . We compare the autocorrelation (coefficient) function estimated from fBm sim-  
 110 ulation ( $\square$ , see below) with eq. (20) (solid line) in fig. 5, where  $\ell = 200$  points. Graphically,  
 111 eq. (20) provides a very good prediction with numerical simulation. Based on this model, it  
 112 is not difficult to find that  $\Gamma_o(\ell) \sim \ell^{2H}$  when  $0 < H < 1$ , corresponding to  $1 < \beta < 3$ , and  
 113  $\tau_o(\ell) = \ell$  when  $0 < H < 0.5$ , corresponding to  $1 < \beta < 2$ . One can find that the validation  
 114 range of scaling exponent  $\beta$  is only a subset of Wiener-Khinchin theorem.

115 We then check the power law for the minimum value of the autocorrelation function  
 116 given in eq. (12). We simulate 100 segments of fractional Brownian motion with length  $10^6$   
 117 data points each, by performing a Wavelet based algorithm [10]. We take db2 wavelet with  
 118  $H = 1/3$  (corresponding to the Hurst number of turbulent velocity). We plot the estimated  
 119 minima value  $\Gamma_o(\ell)$  (+) of the autocorrelation function in fig. 6. A power law behaviour

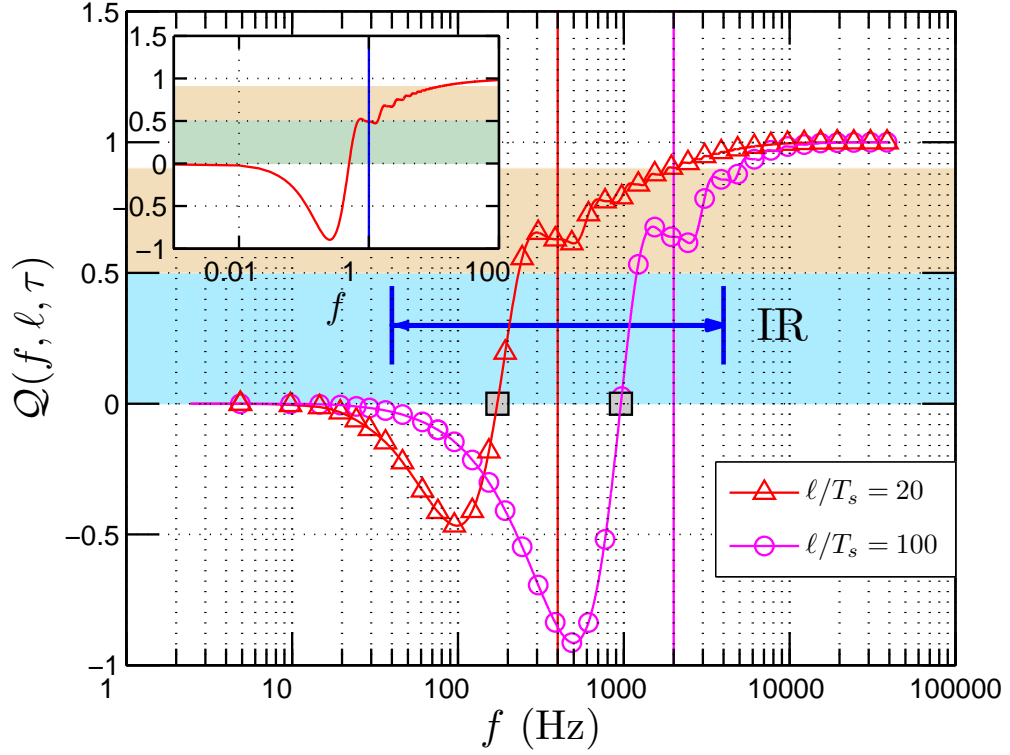


Fig. 7: Cumulative function  $\mathcal{Q}(f, \ell, \tau)$  estimated from turbulent experimental data for spanwise (transverse) velocity with  $\tau = \ell$  in the inertial range, where the numerical solution is shown as inset with  $\ell = 1$ . The inertial range is denoted as IR. Vertical solid lines demonstrate the corresponding scale in spectral space.

120 is observed with the scaling exponent  $\beta - 1 = 2/3$  as expected. It confirms eq. (12) for  
121 fBm. We also plot  $\Gamma_o(\ell)$  estimated from turbulent experimental data for both streamwise  
122 (longitudinal) ( $\square$ ) and spanwise (transverse) ( $\circ$ ) velocity components in fig. 6, where the  
123 inertial range is marked by IR. Power law is observed on the corresponding inertial range  
124 with scaling exponent  $\beta - 1 = 0.78 \pm 0.04$ . Due to the intermittency, this scaling exponent  
125 is larger than  $2/3$ . The exact relation between this scaling exponent with intermittent  
126 parameter should be investigated further in future. The power law range is almost the same  
127 as the inertial range estimated by Fourier power spectrum. It indicates that autocorrelation  
128 function can be used to determine the inertial range. Indeed, as we show later, it seems to  
129 be a better inertial range indicator than structure function.

130 **Discussion.** – We define a cumulative function

$$\mathcal{Q}(f, \ell, \tau) = \frac{\int_0^f K(f', \ell, \tau) df'}{\int_0^{+\infty} K(f', \ell, \tau) df'} \quad (21)$$

131 where

$$K(f, \ell, \tau) = E_{\Delta}(f) \cos(2\pi f\tau) \quad (22)$$

132 is the integration kernel of eq. (8). It measures the contribution of the frequency from 0 to  
133  $f$  at given scale  $\ell$  and time delay  $\tau$ . We are particularly concerned by the case  $\tau = \ell$ . To  
134 avoid the effects of the measurement noise, see fig. 1, we only consider here the spanwise  
135 (transverse) velocity. We show the estimated  $\mathcal{Q}$  in fig. 7 for two scales  $\ell/T_s = 20$  ( $\circ$ ) and  
136  $\ell/T_s = 100$  ( $\triangle$ ) in the inertial range, where the vertical solid line illustrates the location of



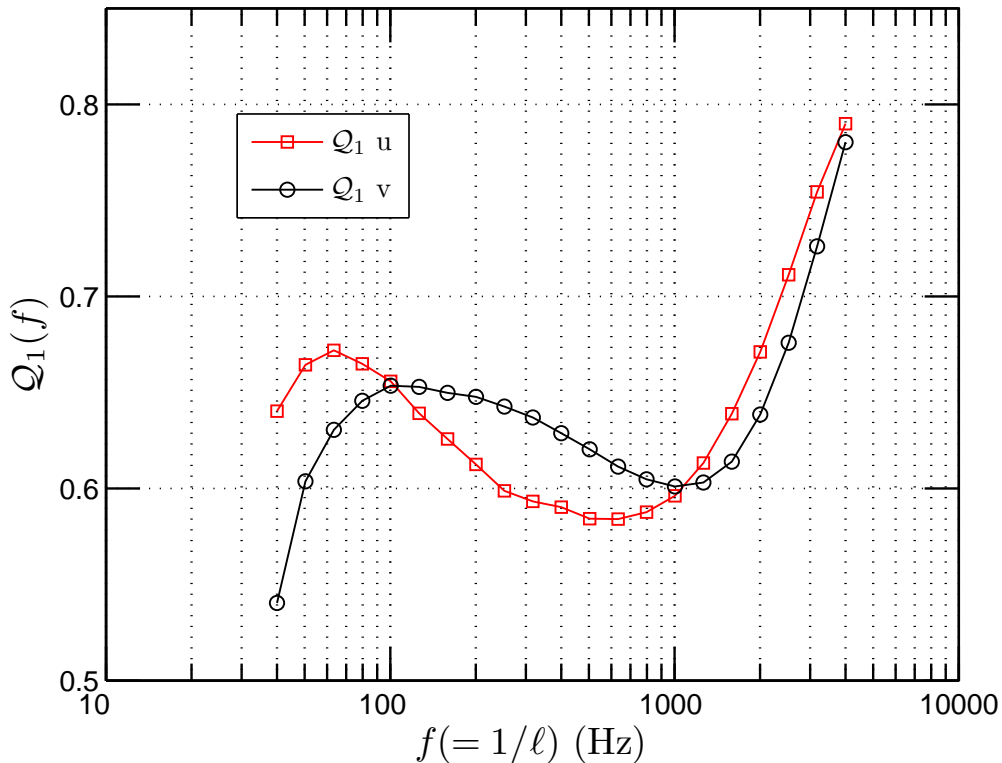


Fig. 8: Cumulative function  $\mathcal{Q}_1(f)$  estimated from turbulent experimental data for both streamwise (longitudinal) and spanwise (transverse) velocity with various  $\ell$ . The numerical solution is  $\mathcal{Q}_1 \simeq 0.5$ .

137 the corresponding time scale in spectral space. In these experimental curves, the kernel  $K$   
 138 given in eq. (21) is computed using the experimental spectrum  $E_v(f)$ . The corresponding  
 139 inertial range is denoted by IR. We also show the numerical solution of eq. (21) with  $\ell = 1$   
 140 as inset, which is estimated by taking a pure power law  $E_v(f) \sim f^{-\beta}$  in eq. (21). We notice  
 141 that both curves cross the line  $\mathcal{Q} = 0$ . We denote  $f_o$  such as  $\mathcal{Q}(f_o) = 0$ . It has an advantage  
 142 that the contribution from large scale  $\ell > 1/f_o$  is canceled by itself. Graphically, in the  
 143 inertial range, the distance between  $f_o$  and the corresponding scale  $\ell$  is less than 0.3 decade.  
 144 The numerical solution indicates that this distance is about 0.3 decade. We then separate  
 145 the contribution into a large scale part and a small scale part. We denote the contribution  
 146 from the large scale part as  $\mathcal{Q}_1(f) = \mathcal{Q}(1/\ell, \ell, \ell)$ . The experimental result is shown in fig. 8  
 147 for both streamwise (longitudinal) and spanwise (transverse) velocity components. The  
 148 mean contribution from large scale is found graphically to be 0.64. It is significantly larger  
 149 than 0.5, the value indicated by the numerical solution. It means that the autocorrelation  
 150 function is influenced more by the large scale than by the small scale.

151 We now consider the inertial range provided by different methods. We replot the cor-  
 152 responding compensated spectra estimated directly by Fourier power spectrum (solid line),  
 153 the second order structure function ( $\square$ ), the autocorrelation function ( $\circ$ ) and the Hilbert  
 154 spectral analysis ( $\triangle$ ) [11] in fig. 9 for streamwise (longitudinal) velocity. For comparison con-  
 155 venience, both the structure function and the autocorrelation function are converted from  
 156 physical space into spectral space by taking  $f = 1/\ell$ . For display convenience, these curves  
 157 are vertically shifted. Graphically, except the structure function, the other lines demonstrate  
 158 a clear plateau. As we have pointed above, the autocorrelation function is a better indicator  
 159 of the inertial range than structure function. We also notice that the inertial range provided

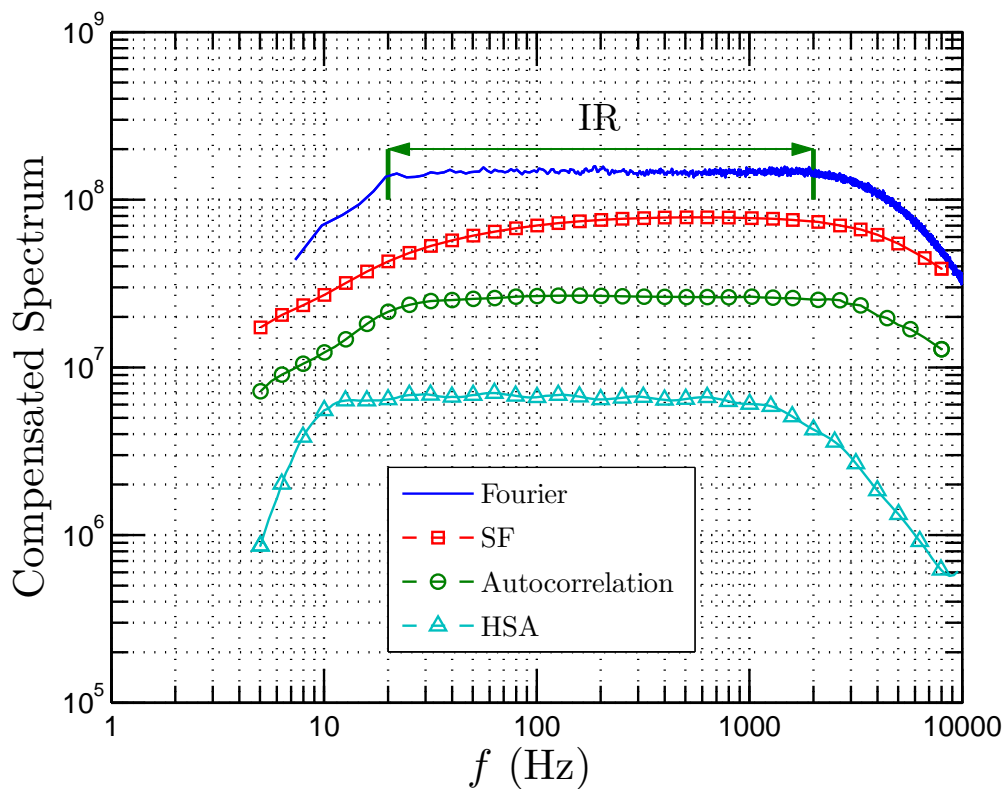


Fig. 9: Comparison of the inertial range for the streamwise (longitudinal) velocity. They are estimated directly by the Fourier power spectrum, the second order structure function, the Hilbert spectral analysis and the autocorrelation function.

160 by the Hilbert methodology is slightly different from the Fourier spectrum. This may come  
 161 from the fact that the former methodology has a very local ability both in physical and  
 162 spectral domain [11, 12], thus the large scale effect should be constrained. However, the  
 163 Fourier analysis requires the stationary of the data, which is obviously not satisfied by the  
 164 turbulence data. The result we present here can also be linked with intermittency property  
 165 of turbulence: we will present this in future work.

166 **Conclusion.** – In this work, we considered the autocorrelation function of the velocity  
 167 increment  $\Delta u_\ell(t)$  time series, where  $\ell$  is a time scale. Taking statistical stationary assump-  
 168 tion, we propose an analytical model of the autocorrelation function. With this model, we  
 169 proved analytically that the location of the minimum autocorrelation function is exactly  
 170 equal to the separation time scale  $\ell$  when the scaling of the power spectrum of the original  
 171 variable belongs to the range  $0 < \beta < 2$ . In fact, this property was found experimentally  
 172 to be valid outside the scaling range, but our demonstration here concerns only the scaling  
 173 range. This model also suggests a power law expression for the minimum autocorrela-  
 174 tion  $\Gamma_o(\ell)$ . Considering the cumulative integration of the autocorrelation function, it was  
 175 shown that the autocorrelation function is influenced more by the large scale part. Finally  
 176 we argue that the autocorrelation function is a better indicator of the inertial range than  
 177 second order structure function. These results have been illustrated using fully developed  
 178 turbulence data; however, they are of more general validity since we only assumed that the  
 179 considered time series is stationary and possesses scaling statistics.

\* \* \*

180 This work is supported in part by the National Natural Science Foundation of China  
181 (No.10772110) and the Innovation Foundation of Shanghai University. Y.H. is financed  
182 in part by a Ph.D. grant from the French Ministry of Foreign Affairs. We thank Nicolas  
183 Perpète for useful discussion. Experimental data have been measured in the Johns Hopkins  
184 University's Corrsin wind tunnel and are available for download at C. Meneveau's web page:  
185 <http://www.me.jhu.edu/~meneveau/datasets.html>.

186 REFERENCES

- 187 [1] KOLMOGOROV A. N., *Dokl. Akad. Nauk SSSR* , **30** (1941) 299.  
188 [2] MONIN A. S. and YAGLOM A. M., *Statistical fluid mechanics* (MIT Press Cambridge, Mass)  
189 1971.  
190 [3] FRISCH U., *Turbulence: the legacy of AN Kolmogorov* (Cambridge University Press) 1995.  
191 [4] ANSELMET F., GAGNE Y., HOPFINGER E. J. and ANTONIA R. A., *J. Fluid Mech.* , **140** (1984)  
192 63.  
193 [5] KANG H., CHESTER S. and MENEVEAU C., *J. Fluid Mech.* , **480** (2003) 129.  
194 [6] PERCIVAL D. and WALDEN A., *Spectral Analysis for Physical Applications: Multitaper and*  
195 *Conventional Univariate Techniques* (Cambridge University Press) 1993.  
196 [7] SAMORODNITSKY G. and TAQQU M., *Stable Non-Gaussian Random Processes: stochastic mod-*  
197 *els with infinite variance* (Chapman & Hall) 1994.  
198 [8] MALIK S. and ARORA S., *Mathematical Analysis* (John Wiley & Sons Inc) 1992.  
199 [9] BIAGINI F., HU Y., OKSENDAL B. and ZHANG T., *Stochastic calculus for fractional Brownian*  
200 *motion and applications* (Springer Verlag) 2008.  
201 [10] ABRY P. and SELLAN F., *Appl. Comput. Harmon. Anal.* , **3** (1996) 377.  
202 [11] HUANG Y., SCHMITT F. G., LU Z. and LIU Y., *Europhys. Lett.* , **84** (2008) 40010.  
203 [12] HUANG Y., SCHMITT F. G., LU Z. and LIU Y., *Traitement du Signal (in press)* , (2009) .